Instrument Responses of Digital Seismographs at Borovoye, Kazakhstan by Inversion of Transient Calibration Pulses

Won-Young Kim
Lamont-Doherty Earth Observatory of Columbia University
Palisades, NY 10964

Göran Ekström
Department of Earth and Planetary Sciences
Harvard University
Cambridge, MA 02138

January 1995

Abstract

A method is developed to determine the response of digital seismographs from transient calibration pulses when there is no recourse to direct measurements. Based on linear system theory, the digital seismograph is represented by a set of first- and higher-order linear filters characterized by their cutoff frequencies and damping coefficients. The transient calibration pulse is parameterized by a set of instrument constants, and the problem is linearized for small perturbations of the constantes with respect to their nominal values. The observed calibration pulse shape is matched in the time domain using an iterative linearized inverse technique. The method is used to derive complete instrument responses for digital seismographs operating at the Borovoye Observatory (BRVK) in Kazakhstan, for which previously only the amplitude responses have been determined. To test the method, we apply it to calibration pulses from a modern digital seismograph system at Kislovodsk (KIV) in northern Caucasus, Russia, and obtain good agreement between known and derived instrument constants. The results of the calibration pulse shape inversion for these seismographs indicate that the method is efficient and that the results are reliable even when microseismic noise is present in the recorded transient calibration pulse. The derived parameters make possible improved quantitative waveform analysis of digital seismograms recorded at BRVK.

1. Introduction

In recent years, the main efforts in the analysis of seismic signals have been directed toward utilizing the full broadband signal, and quantitative interpretation of details in the waveforms for characterization of seismic sources and Earth structure (*efi gfi* Harvey and Choy, 1982; Choy and Cormier, 1983). These types of studies require good knowledge of the response of the instrument on which the seismic signals are recorded. Recently, digital seismograms recorded at the station Borovoye (BRVK), in northern Kazakhstan became available to the seismological community (see Richards *et alfi* 1992). The digital seismograms recorded at BRVK are of high quality owing to the very low microseismic noise at this site, and careful operation. Digital recording at BRVK began in 1966, and the station is important because of its geographical location, and as one of the few digital seismic stations operating in the late 1960s to early 1970s. Efforts are now under way to copy the archive of digital data collected at BRVK, and making these data available to the seismological community.

In order to make full use of this dataset, an important issue is the availability and the quality of response information for the different instruments which have been, and continue to be, operated at BRVK. The goal of this paper is to provide new and more complete response information than has previously been available for one of the seismograph systems operated at BRVK. To obtain such information, we develop a new waveform inversion method for determining the responses of the digital seismographs from their calibration pulses, and apply it to a set of pulses collected at BRVK.

Several methods have been used to determine instrument constants from the calibration pulse. For the World Wide Standardized Seismograph Network (WWSSN) seismographs, whose records have been extensively used by many researchers since the early 1960s, the instrument constants have been determined from the analog calibration pulse and the instrument response is obtained using the theoretical formula given by Hagiwara (1958). Mitchell and Landisman (1969) used a least-squares inversion of the calibration pulse to determine the

instrument constants for the WWSSN long-period seismographs. Jarosh and Curtis (1973), McGonigle and Burton (1980) and Mitronovas (1976), among others, extended the method of Mitchell and Landisman (1969) to reduce the uncertainties of the instrumental constants which, in turn, reduced significantly the uncertainties of the overall responses, particularly the phase delay.

For the Global Digital Seismograph Network (GDSN), which includes the Seismic Research Observatory (SRO), Modified High-Gain Long-Period (ASRO) and International Deployment of Accelerometers (IDA) seismographs operating since 1977, the instrument responses were obtained by several researchers. Using the circuit diagrams and employing linear control system theory, Luh (1977), McCowan and Lacoss (1978), Berger *et alfi*(1978) and Farrell and Berger (1979), among others, obtained transfer functions of the GDSN long- and short-period seismographs. Herrmann (1977) obtained the impulse response of the SRO long-period seismograph by differentiating its step acceleration calibration pulse in the time domain and derived the phase response from the amplitude response via the Hilbert transformation (Bolduc *et alfi* 1972), assuming a minimum-phase causal system.

The approach that we have chosen to pursue in this paper is a pragmatic one. For seismographs at Borovoye, the complete circuitry and seismogram system design is not available, and therefore a complete, theoretical response cannot be derived. However, limited information exists, such as nominal values of seismometer period and damping, recordings of impulse response pulses, and high-quality amplitude calibrations for several frequencies. We therefore attempt to make reasonable assumptions about what physical components make up each system, and then proceed to adjust the parameters which describe these components in such a way that agreement is found between observed and predicted calibration information. This approach will in general not yield a unique set of parameters, but we are less interested in the true instrument constants than we are in predicting the complex response curve over the frequency range that the seismograph has significant sensitivity. The advantage of our approach over an entirely empirical one, such as Herrmann's (1977), is that a parameterized approach is much less sensitive to noise in the calibration signal, and that the response function which results is easily represented in terms of poles, zeros, and a gain.

2. Theory and Method

A digital seismograph generally consists of a sensor, a low-pass anti-aliasing filter, an analog-to-digital (A/D) converter, and a recorder. Assuming the magnitude of input ground motion is small, the instrument response can be conveniently analyzed by employing linear system theory (*efigfi*D'Azzo and Houpis, 1975). Although modern digital seismographs are complicated by the extensive electronic circuitry involved, most systems can be represented by a linear combination of first-, and higher-order filters, which in turn are characterized by their corner frequencies (f_c) and damping coefficients (ξ) (see *efigfi*Graupe, 1972; Farrell and Berger, 1979). The net response is obtained by the product of all elements. A general linear system transfer function, $F(s)$, can be described as a ratio of polynomials (*efigfi*D'Azzo and Houpis, 1975),

$$F(s) = K\frac{a_0 + a_1 s + a_2 s^2 + \cdots + a_n s^n}{b_0 + b_1 s + b_2 s^2 + \cdots + b_m s^m} = K\frac{N(s)}{D(s)} \tag{1}$$

or in its factored form,

$$F(s) = K' \frac{(s - z_1)(s - z_2) \cdots (s - z_n)}{(s - p_1)(s - p_2) \cdots (s - p_m)} = K' \frac{\prod_{i=1}^{N}(s - z_i)}{\prod_{j=1}^{M}(s - p_j)} \tag{2}$$

where K and K' are constants, z_i and p_j are the complex zeros and poles of $F(s)$, and $s = i\omega$ is the Laplace transform variable.

For example, a pendulum seismometer is a linear second-order system, which has a simple response transfer function (*efi gfi*Aki and Richards, 1980) which when written as a Laplace transform becomes

$$F(s) = K \frac{-s^2}{s^2 + (2\xi\omega_0)s + \omega_0^2} \tag{3}$$

where ξ is the damping constant and ω_0 is the free angular frequency of the pendelum. The denominator in equation (3) has two roots, which are the poles of the response function. The numerator has two roots at the origin, which are the zeros of the response function.

For a pendulum seismometer, the only parameters which need to be determined are the magnification, the free period, and the damping. For slightly more complex systems with additional low- and high-pass filters, the cut-off period, damping and order of each filter are additional unknowns. Often the order of low- and high-pass filters can be deduced from the amplitude response fall-off at high and low frequencies, reducing the number of unknown parameters.

Given a description of the seismograph system in terms of its components, its impulse response can be computed and compared with an observed calibration pulse. If the parameters describing the system are accurate, the two pulses will agree; if not, the system parameters need to be adjusted. The shape of the calibration pulse is a non-linear function of the cutoff frequencies and damping coefficients. However, we can linearize the problem for small perturbations in the instrument constants. The system response can then be modified by iterative perturbation of the instrument parameters, away from an initial estimate of the nominal values.

If the theoretical calibration pulse corresponding to an estimate of the system parameters p_i is $u(t; p_i)$, the effect of a small perturbation, δp_i is

$$\delta u(t; p_i) = u(t; p_i + \delta p_i) - u(t; p_i) \tag{4}$$

where i is an index referring to the i-th parameter. The synthetic calibration pulse in each iteration is calculated in the frequency domain using equation (2), and then inverse Fourier transformed. Figure 1 shows the perturbations, $\delta u_i(t; p_i)$, calculated for the TSG-KSM short-period seismograph at BRVK, discussed in next section, from its nominal values and a 5 % perturbation of each instrument constant.

Once the kernels $\delta u_i(t; p_i)$ are calculated, the inverse problem is formulated which in a least-squares sense minimizes the difference between the observed and synthetic calibration pulses. The misfit function $\Psi(p_i)$ is

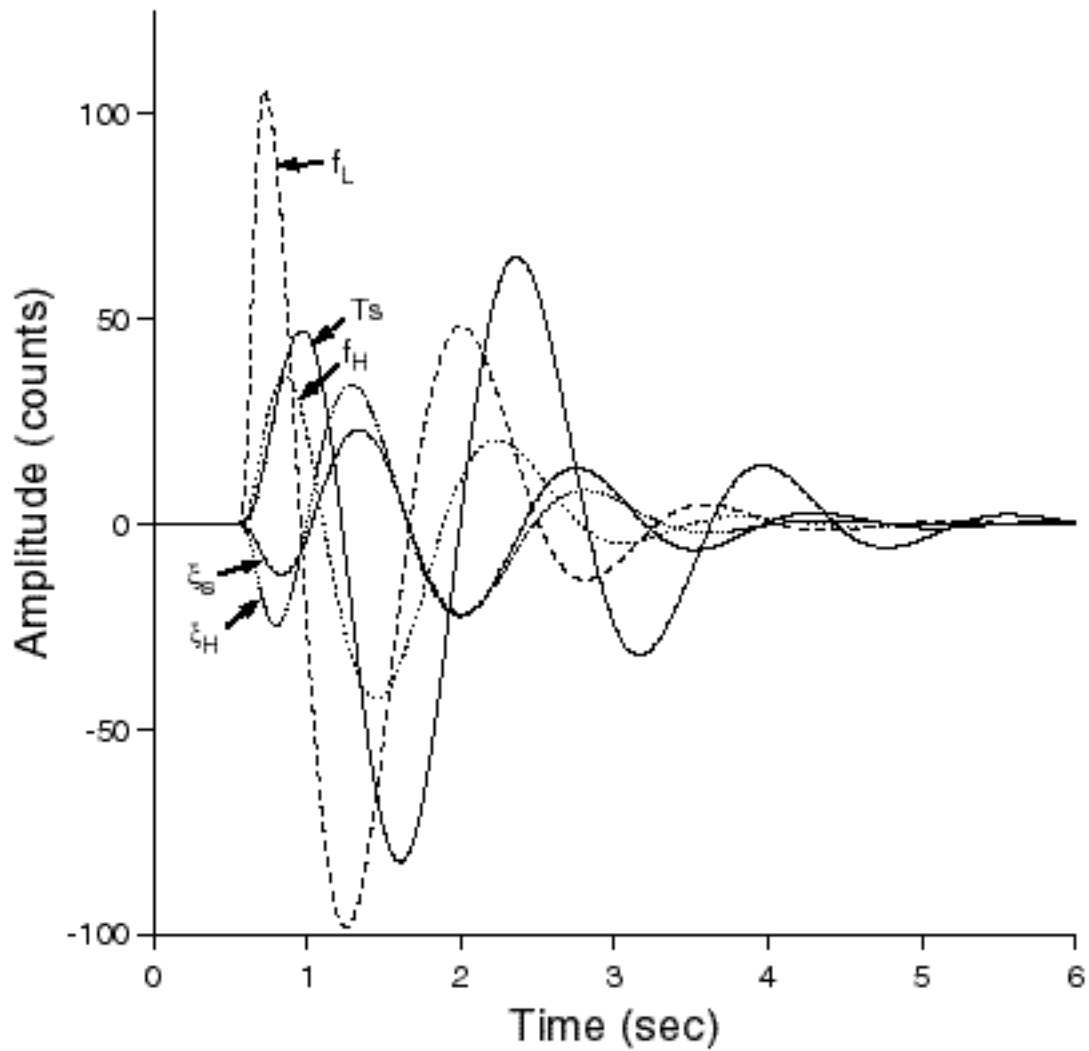$$\Psi(p_i) = \left[\frac{1}{J} \sum_{j=1}^{J} (O_j - C_j(p_i))^2 \right]^{1/2}, \tag{5}$$

Figure 1: Kernel waveforms corresponding to small perturbations (+5%) of the parameters for the calibration pulse of the TSG-KSVM seismograph. Perturbations of individual parameter are plotted for small perturbations with respect to seismometer natural period (*thick solid line*), seismometer damping (*thin solid line*), the second-order high pass filter cutoff frequency (*thick dotted line*), and damping (*thin dotted line*), and third-order Butterworth low-pass filter cutoff frequency (*dashed line*).

where O_j is the observed time series, $C_j(p_i)$ is the calculated time series, the sum is over digital samples, and J is the number of samples used in the inversion. The parameter changes obtained in the inversion are added to the starting model and further iterations are performed until the process converges.

In this minimization procedure there are sometimes perturbations in cutoff frequencies and damping constants which produce very similar changes in the calibration pulse, leading to instabilities in the inversion. We have found that a useful way to eliminate these instabilities is to reparameterize the problem with fewer unknown variables, for example by fixing one of the poorly constrained parameters to its nominal value.

In addition to the parameters discussed thus far, the amplitude of the recorded calibration pulse also depends on the magnitude of the current being fed through the calibration coil, and the coil constant. In our application, neither of these parameters is known, and we include an amplitude factor K as an additional parameter in our inversion. The initial value of K is calculated from the ratio of the recorded calibration pulse to the initial theoretical pulse, but is then solved for in the inversion. For some the calibration pulses, there are significant offsets in the calibration curve. In these cases, the synthetic pulse is aligned with the recorded pulse by adjusting the baseline, which is the difference between the mean of the two pulses (Mitchell and Landisman, 1969).

In summary, the iterative inversion for system parameters proceeds in four steps: 1) recorded and synthetic calibration pulses are aligned in time and baseline adjusted; 2) kernels for the inversion is formed as in equation (4); 3) corrections to the parameter values are found from the linearized inversion; 4) parameters are updated. These steps are repeated until convergence is achieved.

3. Application

We determined the responses of digital seismographs at the station Borovoye (BRVK) in northern Kazakhstan using the method described in the previous section. Since 1965 there has been several digital seismograph systems operated at BRVK. Each seismograph system has its own seismometers and recording devices (see Richards *et alfi* 1992). In this study, we analyze the responses of the various seismographs of STsR-TSG system (hereafter referred to as TSG), which has been in operation since February 1973, and has proved to be one of the better systems at BRVK (Table 1).

The TSG seismograph system has two 3-component, short-period (KS and KSM) and two 3-component, long-period (DS and DSM) seismometers and a vertical-component short-period seismometer (KSVM). The seismic signals from all short- and long-period seismometers are digitized with 11 bit A/D conversion. Digitized two-byte samples are multiplexed and recorded digitally on a magnetic tape. The signals from all seismometers, except the basic KS and DS seismometers, are recorded both in low- and high-gain modes, which increases the overall dynamic range of the system, otherwise limited by the 11 bit digitizing. A total of 24 channels of digital records are written on a wideband 17-track tape.

Nominal instrument constants of these seismographs were obtained from; 1) seismometer free period, damping and overall digital sensitivity (in counts/μ) given in Adushkin and An (1990); 2) analysis of frequency-amplitude calibration tables of the TSG system available at the Borovoye Observatory. Although it was reported that the TSG system is carefully calibrated every year, only information on the amplitude responses and overall gains and

no phase information were available to us. This appears to be a common situation for seismographs in the former Soviet Union. On a more routine basis, transient calibration pulses are generated and recorded to check the overall digital sensitivity of the system. We obtained digital recordings of such calibration pulses from all seismometers of the TSG system, recorded on February 8, 1988 (15:00). The pulses are generated by feeding a step calibrating signal with duration of 8 msec into the seismometer damping coils. The recorded calibration pulse corresponds to the seismograph response to an impulse in ground acceleration, since the duration of calibrating signal is much shorter than the shortest recorded periods. The recorded calibration pulse is in this case equivalent to the multiplication of the system transfer function for ground displacement by $(i\omega)^{-2}$ (*e.g.* Herrmann, 1977). We parameterized the responses of all seismometers (channels) of the TSG system in terms of cutoff frequencies and damping factors of a set of linear first- and second- and third-order filters. Each filter is parameterized by a cutoff frequency, f_c, and damping, (ξ). The subscripts S, H or L are used to indicate seismometer, high- or low-pass filters, respectively, and integer subscripts, such as 1, 2, or 3, are used to indicate the order of the filters. The transfer functions of each seismograph obtained from the inversion are then easily represented by complex poles and zeros in the complex s-plane, which are convenient for further analysis of observed records. In the following subsections, we describe the analysis of the available calibration pulses.

2.2 Short-Period Seismographs

The signals from the TSG system short-period seismometers are recorded with a sampling interval of 26 msec. Of the three short-period systems in operation at BRVK, we were able to fully analyze the KSM amd KSVM systems. Calibration pulses for the KS seismograph were clipped.

TSG-KS Seismograph The KS seismograph is the basic 3-component, short-period instrument of the TSG system. This instrument has a nearly flat response to ground displacement in the frequency band 0.7–5 Hz (-3 db level) and has a nominal gain of 4500 counts/μ at 1.5 Hz (Table 1). Unfortunately, calibration pulses for all three components of this seismograph were clipped, and we were therefore unable to derive complete transfer functions for this seismograph. We present nominal values for this instrument in Table 3, based on Adushkin and An's (1990) values for the seismometer, and our estimate of additional filter parameters from the shape of the amplitude calibration curves.

TSG-KSM Seismograph The 3-component, short-period KSM seismometers have stronger magnets than the basic KS model, allowing twice the gain. The KSM high-gain channels have a low-noise amplifier and are the most sensitive short-period channels (sensitivity 100,000 counts/μ at 1 Hz) at BRVK. The KSM short-period instrument also records on low-gain channels, with a nominal gain of 1000 counts/μ at 1 Hz. The low-gain channels ensure on-scale recordings of strong seismic signals which may saturate the high-gain channels. Hence, the KSM short-period instrument provides overall dynamic range of about 100 db — 60 db on the low- and high-gain channels with 11 bit digitizing, and about 20 db overlap across the gain levels. After some preliminary analysis of the amplitude response curve, we inferred that the KSM seismograph can be considered to consists of a seismometer, a second-order high-pass filter, and a third-order Butterworth low-pass filter (Figure 2). We parameterized the inverse problem in terms of the seismometer free period and damping,

the high-pass filter corner and damping, and the low-pass corner period. If part of a linear system response can be represented by a Butterworth or Bessel filters, it reduces the number of parameters in the inversion significantly, since only a cutoff frequency and an order are needed to represent such a filter.

The recorded calibration pulses are inverted for the five instrument constants and an overall amplitude factor (see also Figure 1). For the vertical component, a stable solution is obtained after three iterations, and results from the three iterations are listed in Table 2. The instrument constants obtained from the best fit waveform inversion for all components are given in Table 3, and comparisons between recorded and synthetic calibration pulses are shown in Figure 3. The final solution shows that instrument constants of all three components have similar values with relatively small deviations from the nominal values. However, for the vertical component the deviation for the seismometer damping is more than 5%.

A comparison between the spectral amplitudes obtained from the time domain calibration pulse inversion and spectral amplitude response of the KSM instrument measured independently is shown in Figure 4. There is excellent agreement between the two measurements of the amplitude responses, indicating that the result of the calibration pulse shape inversion is reliable. The obvious advantage of the inversion in the time domain is that we obtain the phase as well as the amplitude response of the instrument. Comparison with the amplitude calibration data also allows us to establish the total gain of the system. We adjust the constant coefficient K in equation (1) so that there is agreement between the theoretical curve and the amplitude calibrations near the period of peak amplification.

While the agreement between spectral amplitudes in Figure 4 is good, there are some discrepancies at the high frequency end of the amplitude spectra on both horizontal components (Figure 4). The misfits of the amplitude responses are at frequencies greater than about 8 Hz on both horizontal components. The misfits are mainly due to the cutoff frequencies of the third-order Butterworth low-pass filter. It is unclear whether the time domain calibration pulse shape inversion could not fit the high-frequency part of the signal or if the given amplitude calibrations are incorrect. One possibility is that the time domain calibration pulse shape inversion is not fitting the high frequencies ($\geq$ 8Hz) well because of seismic and instrument noise. Between about 8 Hz and the Nyquist freqeuncy, the calibration pulse has very small spectral power, since the impulse acceleration input signal results in a recorded pulse spectrum with ω^{-2} scaling of the displacement response spectrum.

TSGfKSVM Seismograph   The KSVM seismograph is a sensitive short-period instrument with special electronics. The KSVM seismometer also has a stronger magnet than the KS seismometer, allowing twice the gain. This instrument records only vertical-component digital data in two channels; a low-gain (50 counts/μ at 1 Hz) and a high-gain (4600 counts/μ at 1 Hz). Most of the seismic signals from the strong underground nuclear explosions ($m_b(Lg) > 5.5$) at Eastern Kazakhstan Test site (Degelen Mountain, $\Delta = 620$ km and Balapan, $\Delta = 690$ km) are well recorded by the KSVM low-gain channel. The KSVM high-gain channel and the other short-period instruments (KS and KSM) are usually saturated by signals from these strong regional events.

Similarly to the KSM system, the KSVM can be considered to consist of a seismometer, a second-order high-pass filter, and a third-order Butterworth low-pass filter. The instrument
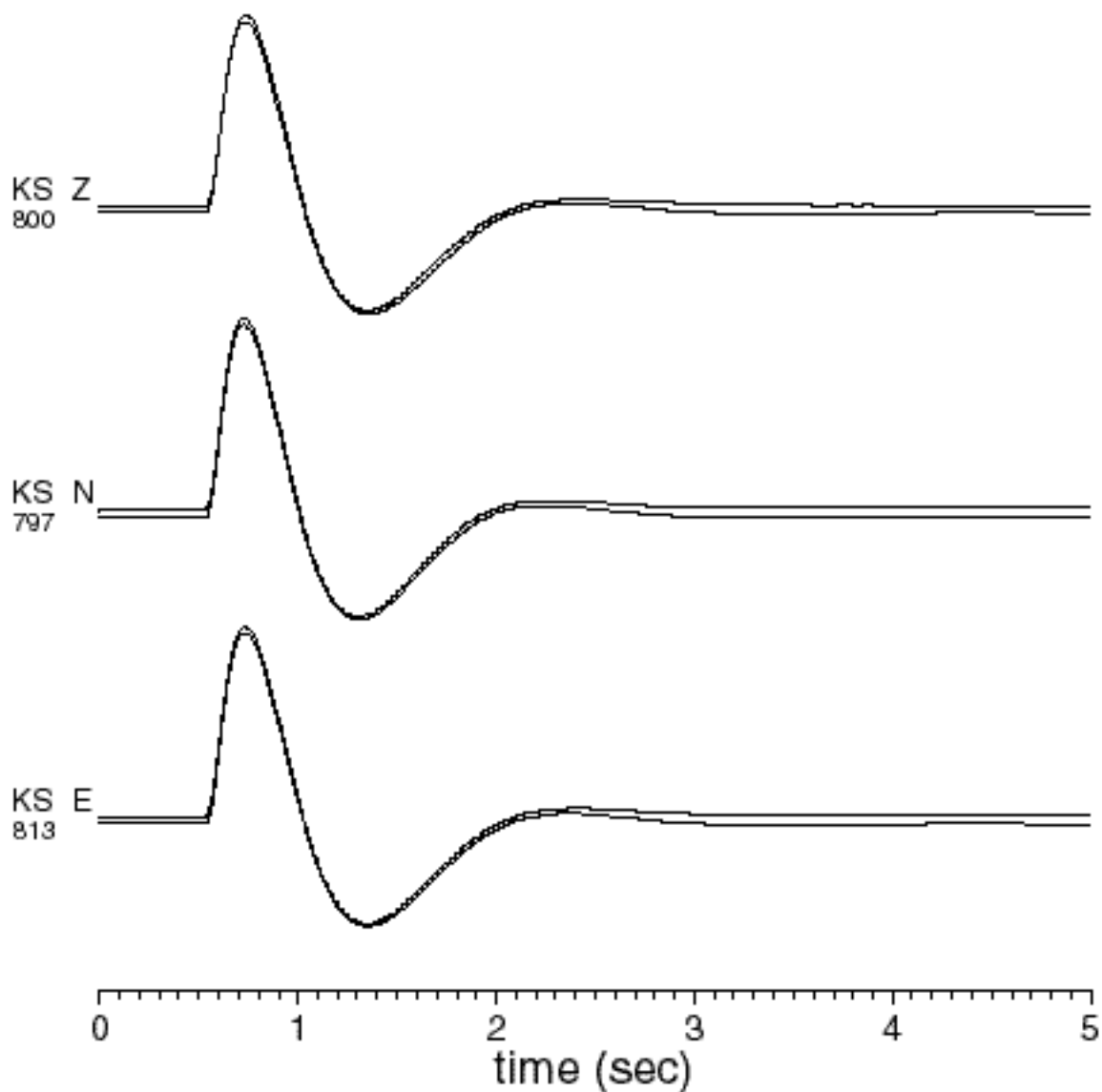
Figure 2: Frequency-amplitude responses of individual elements of the KSVM seismograph are plotted together with the instrument's net response. The elements and their adjustable parameters are: seismometer with natural period and damping (*solid line*); second-order high pass filter with a cutoff frequency and a damping (*dotted line*); a third-order Butterworth low-pass filter with a cutoff frequency (*dashed line*).
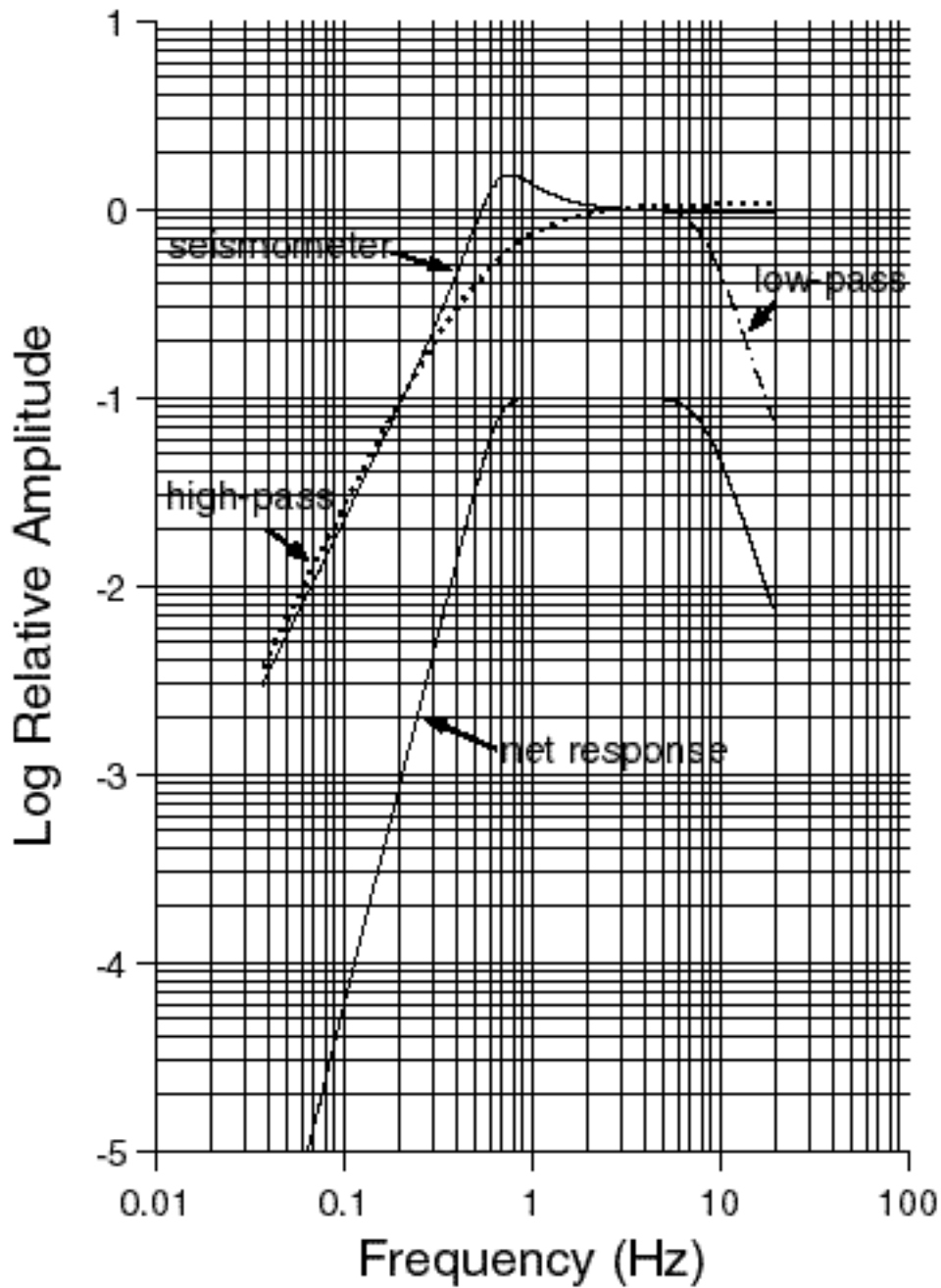
Figure 3: Comparisons between the calibration pulses recorded by the 3-component, short-period KSM seismograph (*thick traces*) and corresponding synthetic calibration pulses after the waveform inversion (*thin traces*). Synthetic pulses calculated with the final instrument constants are plotted with small vertical offsets to show the overall fits.
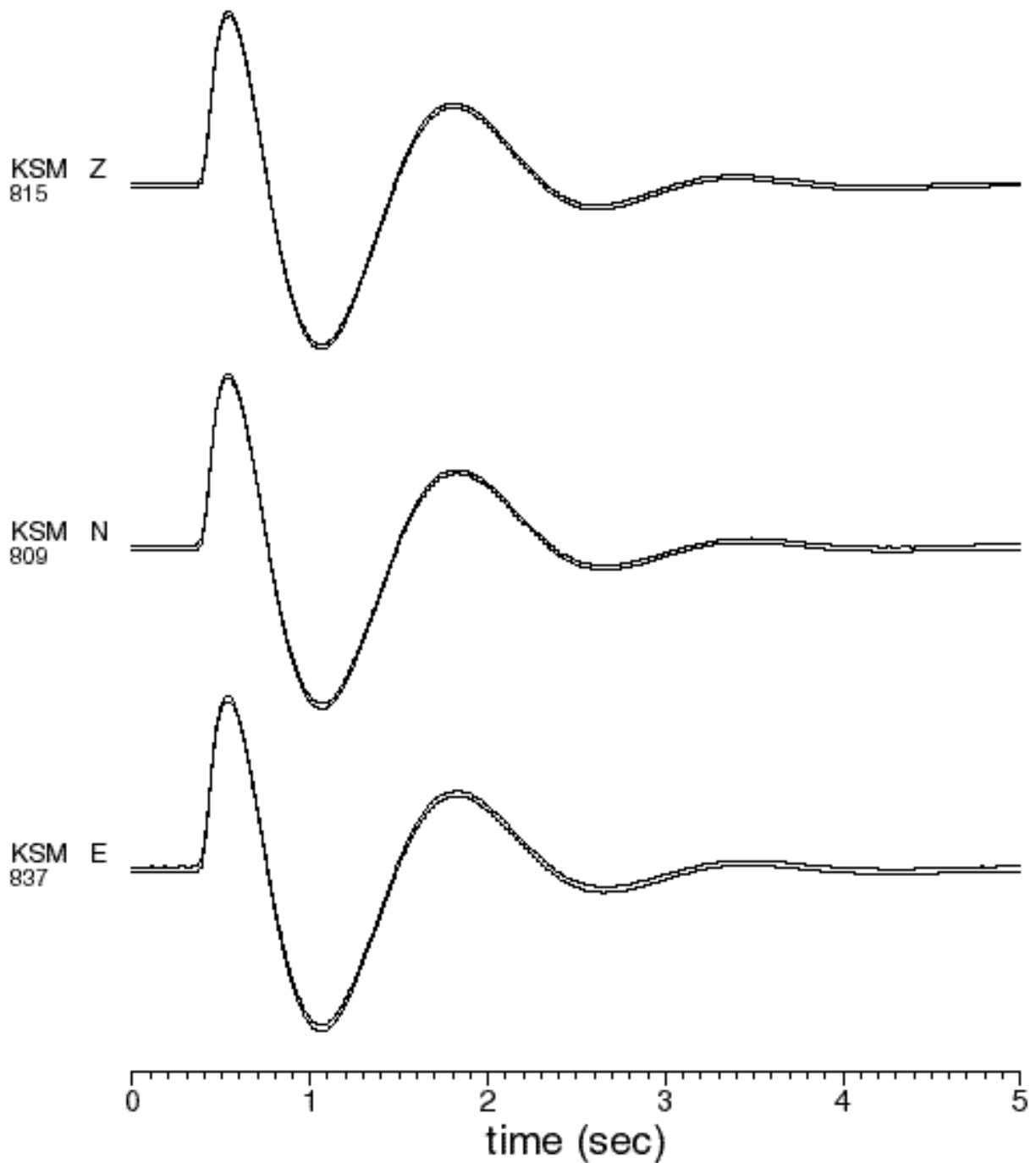
Figure 4: Comparisons between the spectral amplitude responses of the 3-component, short-period KSM seismograph (Z=*closed circles*, N, E=*open circles*) and the amplitude responses obtained after the waveform inversion (Z=*solid line*, N=*dotted line*, E=*dashed line*). Frequency-amplitude responses are measured independently from the calibration pulse. Notice that horizontal components have slightly higher responses than the vertical component.

constants determined from the waveform inversion are given in Table 3 and a comparison between the recorded and the final synthetic calibration pulses are shown in Figure 5. The fits between the observed and the synthetic pulses are good. A comparison between the spectral amplitude response of the KSVM seismograph measured independently and the amplitude responses obtained after the waveform inversion are shown in Figure 6. The waveform inversion yields a response with slightly higher cutoff frequency at about 5.8 Hz. Waveform fits with cutoff frequencies between 5.3 and 5.8 Hz give acceptable solutions considering the presence of higher instrument noise at the high frequency end in the calibration pulse. We choose the solution with a cutoff frequency $f_{L3} = 5.3$ Hz as the final solution.

fiffi Longf Period Seismographs

The signals from long-period seismometers of the TSG system are recorded with a sampling interval of 312 msec. We were able to analyze calibration pulses from both the DS and DSM long-period systems.

TSGf DS Seismograph   The DS seismograph is the basic 3-component, long-period instrument of the TSG system. These long-period channels have nominal gains of 50 counts/μ at about 0.1 Hz. The DS seismograph consists of an underdamped seismometer with 20 sec natural period, a second order high-pass filter, a first-order low-pass filter, and a second order low-pass filter. We invert for four periods and three damping coefficients (assuming that the first-order low-pass filter is a Butterworth), and an overall amplitude factor. All variables are well constrained. The results of the inversion are listed in Table 3, and a comparison between observed and synthetic calibration pulses can be seen in Figure 7. We found that the vertical seismometer has significantly greater damping ($\sim$15%) than the horizontal ones for this system. A comparison between the spectral amplitude responses of the vertical component, long-period DS seismograph from the calibration table and the amplitude responses obtained after the waveform inversion are shown in Figure 8.

TSGf DSM Seismograph   The DSM seismograph is a 3-component, long-period instrument with special electronics. Its seismometer has longer period ($T_S = 28$ sec) and a stronger magnet than the DS seismometer which allows for twice the gain. The DSM instrument records seismic signals in two gain levels; a low-gain channel (nominal gain = 10 counts/μ) at 14 sec) and a high-gain channel (nominal gain = 1000 counts/μ at 14 sec).

The DSM seismograph consists of an underdamped seismometer, two first-order high-pass filters and one third order low-pass filter, which we assume is a Butterworth filter. The inversion is parameterized in terms of six variables. Except for the NS-component, the inversion resolves all parameters well. For the NS-component, we fixed the low-pass cutoff frequency at the value obtained in the analysis for the Z-component.

We find that the seismometer natural periods show about $\pm$5% deviation from the nominal setting, while the seismometer damping varies by about $\pm$4% between the three components. The parameters obtained from the best fit waveform inversion are given in Table 3. A comparison between the spectral amplitude response obtained in this study and the values given in the calibration table is shown in Figure 9. There is a fairly good agreement, but the comparison of only the spectral amplitudes in the frequency domain illustrates that such comparisons fails to detect substantial deviation of instrument response from the nominal response, due to lack of phase information in such measurements.
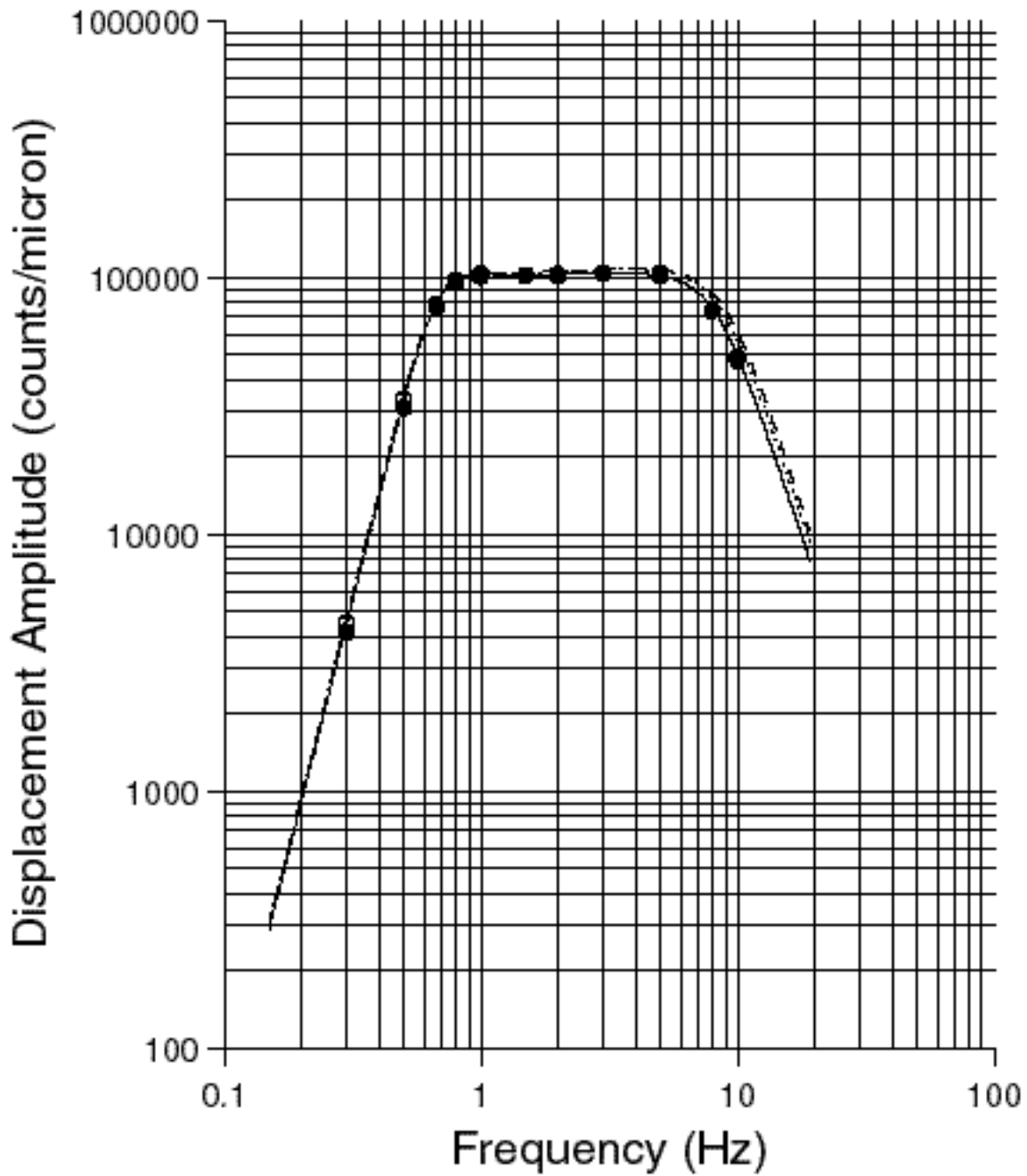
Figure 5: Comparisons between the calibration pulses recorded by the vertical component, short-period KSVM seismograph (*thick traces*) and corresponding synthetic calibration pulses (*thin traces*). Synthetics calculated with nominal instrument constants before the calibration pulse waveform inversion (*upper traces*) and the synthetics after the waveform inversion (*lower traces*) are plotted to show the overall fits.
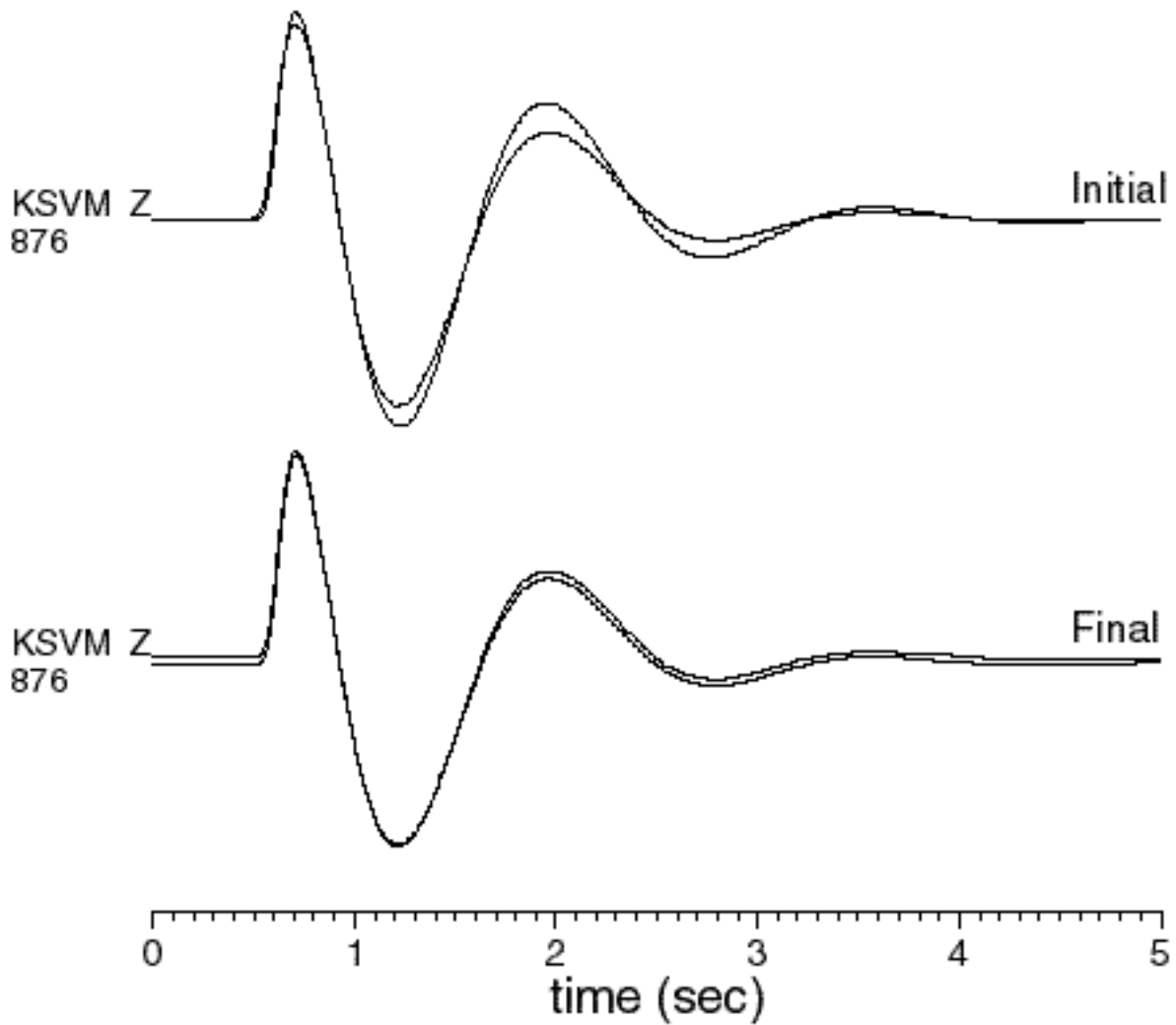
Figure 6: A comparison between the spectral amplitude response of the vertical component, short-period KSVM seismograph (*closed circles*) and the amplitude responses obtained after the waveform inversion (*solid line*). The waveform inversion yields the response with slightly higher cutoff frequency at about 5.8 Hz (*dashed line*). Waveform fits with cutoff frequencies between 5 Hz and 5.8 Hz give acceptable solutions considering the presence of higher instrument noise at the high frequency end in the calibration pulse. Frequency-amplitude responses are measured independently from the calibration pulse.
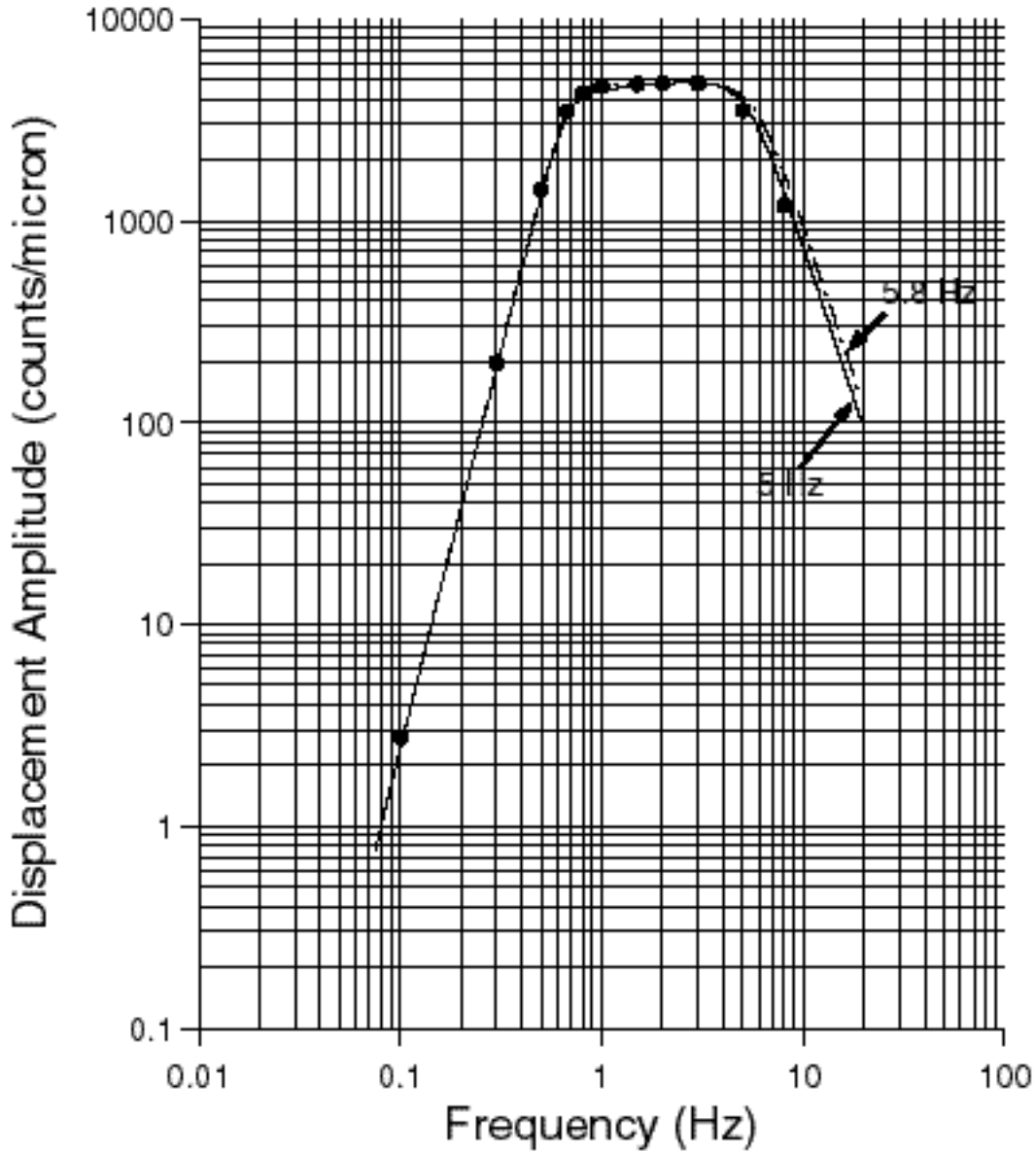
Figure 7: Comparisons between the calibration pulses recorded by the vertical component, long-period DS seismograph (*thick traces*) and corresponding synthetic calibration pulses (*thin traces*). Synthetics calculated with nominal instrument constants before the calibration pulse waveform inversion (*upper traces*) and the synthetics after the waveform inversion (*lower traces*) are plotted to show the overall fits.
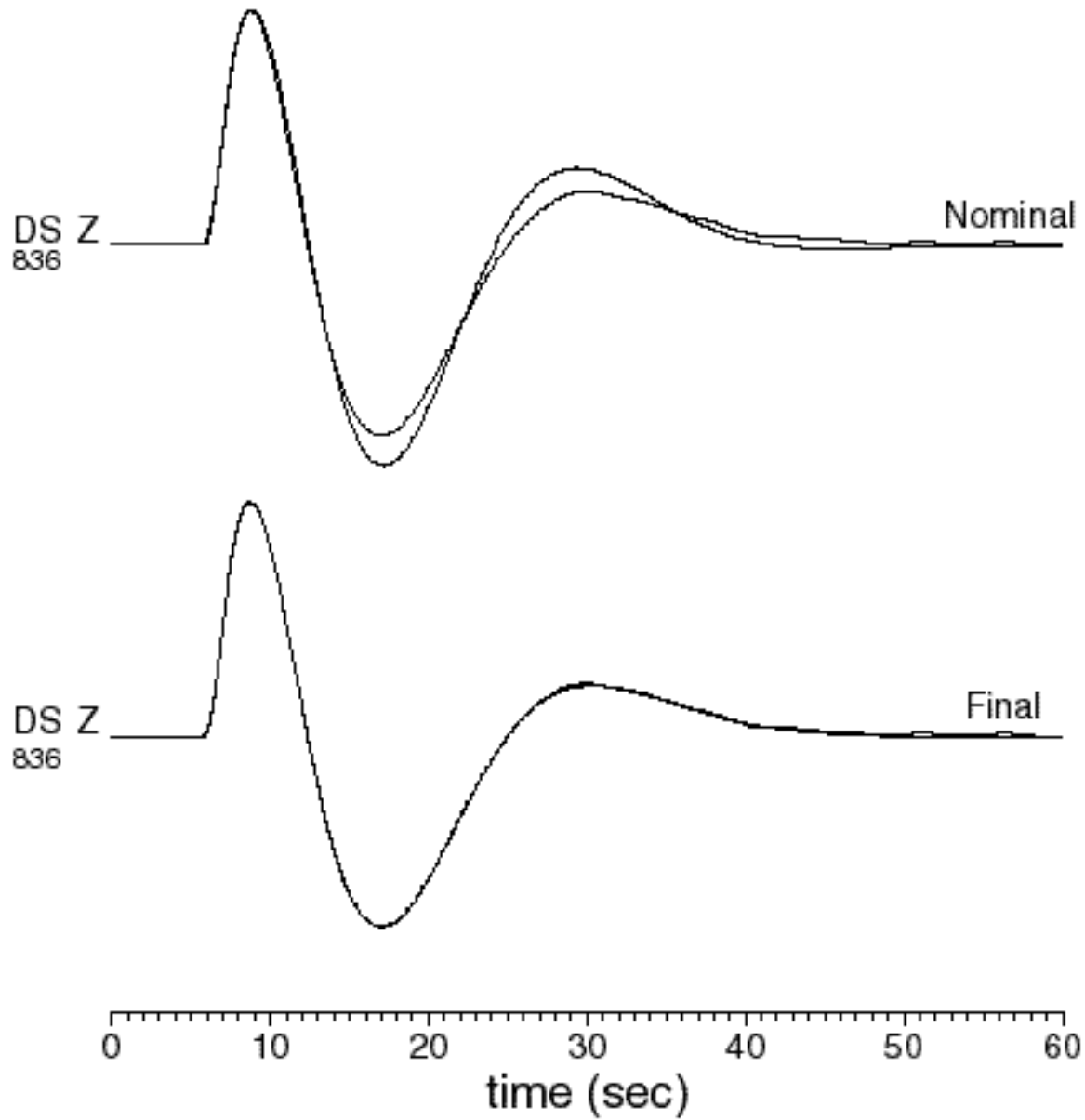
Figure 8: Comparison between the spectral amplitude response of the vertical-component, long-period DS seismograph (*closed circles*) and the amplitude response obtained after the waveform inversion (*solid line*).
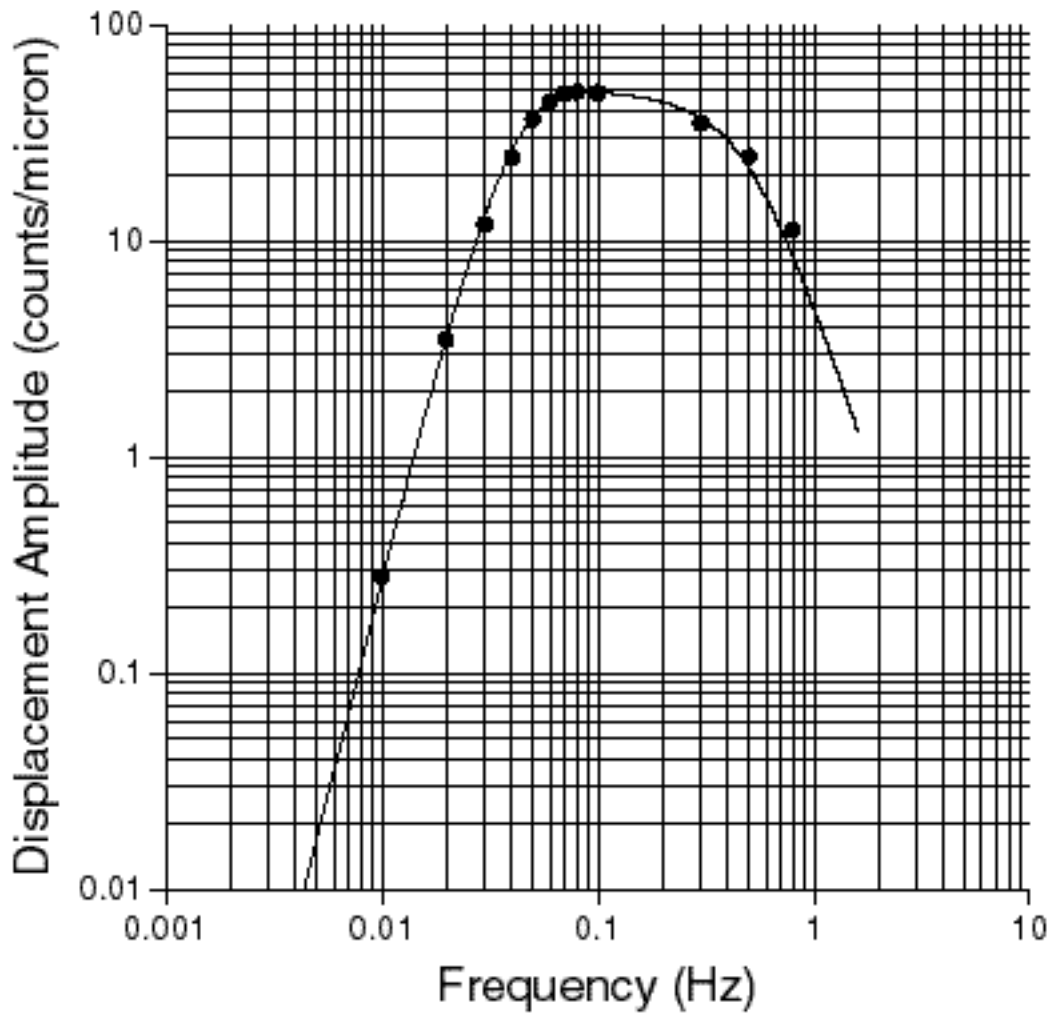
Figure 9: Comparison between the spectral amplitude response of the vertical-component, long-period DSM seismograph (*closed circles*) and the amplitude response obtained after the waveform inversion (*solid line*).

fiffi SVfi Response at KIVfi North Caucasus Network

In the previous sections, the instrument constants of various short- and long- period seismographs at BRVK were determined from the calibration pulse by waveform inversion in the time domain. However, for all seismographs at BRVK, only the nominal values of the seismometer natural periods and dampings were known, and the characteristics of the first- and higher-order filters used were unknown to us. The nominal cutoff frequencies and damping constants of these filters were inferred by us from available frequency-amplitude response information on the seismographs. In order to examine the validity of such inferences, we applied the method proposed in this study to a seismograph whose characteristics are already very well known.

The SV1 seismograph at KIV (Kislovodsk, Russia) is a vertical-component, intermediate-period instrument with SV1 seismometer (Kinemetrics) and a remote digitizer (model RD-3; Nanometrics). The nominal gain is 238.79 V/M/s at 1 Hz. Signals are digitized on site by a 16 bit digitizer (RD-3) at 240 samples/sec through a fifth-order low-pass Butterworth anti-aliasing filter with cutoff frequency at 34.3 Hz. The digital signal is then filtered with a digital finite impulse response (FIR) filter with a factor of four decimation, which provides a 60 samples/sec datastream. The SV1 seismograph consists of; 1) an intermediate-period seismometer with the natural period, $T_s = 5$ sec and damping $\xi_s = 0.707$; 2) a fifth-order Butterworth low-pass filter with cutoff frequency, $f_{L5}=34.3$ Hz; 3) a digital FIR filter with 56 coefficients and a factor of four decimation. The amplitude response of the SV1 seismograph is nearly flat to the input ground velocity in the frequency band 0.2–23.4 Hz. A comparison between the vertical-component, recorded and synthetic calibration pulses are shown in Figure 10. The calibration pulses are generated by applying a Heaviside step current pulse with duration of about 10 sec into the seismometer damping coil.

We parameterize the instrument response of the SV1 seismograph with three instrument constants, an amplitude factor, and 56 digital FIR filter coefficients which are fixed in the inversion. The parameters are well resolved in the inversion, and a stable solution is obtained after 3–4 iteration. A comparison between the recorded calibration pulse and the synthetic calibration pulse after the waveform inversion are shown in Figure 10. The fit between the recorded and synthetic calibration pulses is excellent indicating that the method works well for determining the instrument constants of this more modern digital seismograph system. The parameters obtained from the best fit waveform inversion are given in Table 4. The seismometer natural period shows about -7.8% deviation from the nominal setting, while seismometer damping differ by about +14.4% from the nominal value. It was later confirmed that the seismometer damping indeed was modified to $\xi_s = 0.867$ after the initial installation of the seismograph (D. Lentrichia, personal communication, 1994). A comparison between the spectral amplitudes of the recorded and the synthetic calibration pulses are plotted in Figure 11. There is a fairly good agreement between the two spectral amplitudes up to about 10 Hz, but the spectral amplitudes at frequencies higher than 10 Hz show some differences.

fiffi Example Waveforms from a Deep Focus Earthquake

We have used P wave records from deep focus teleseismic earthquakes to assess the reliability of instrument responses. A comparison between the observed and synthetic vertical and radial component records from a deep focus earthquake that occurred in Southern Honshu, Japan is shown in Figure 12. Observed vertical and East-West component (which is
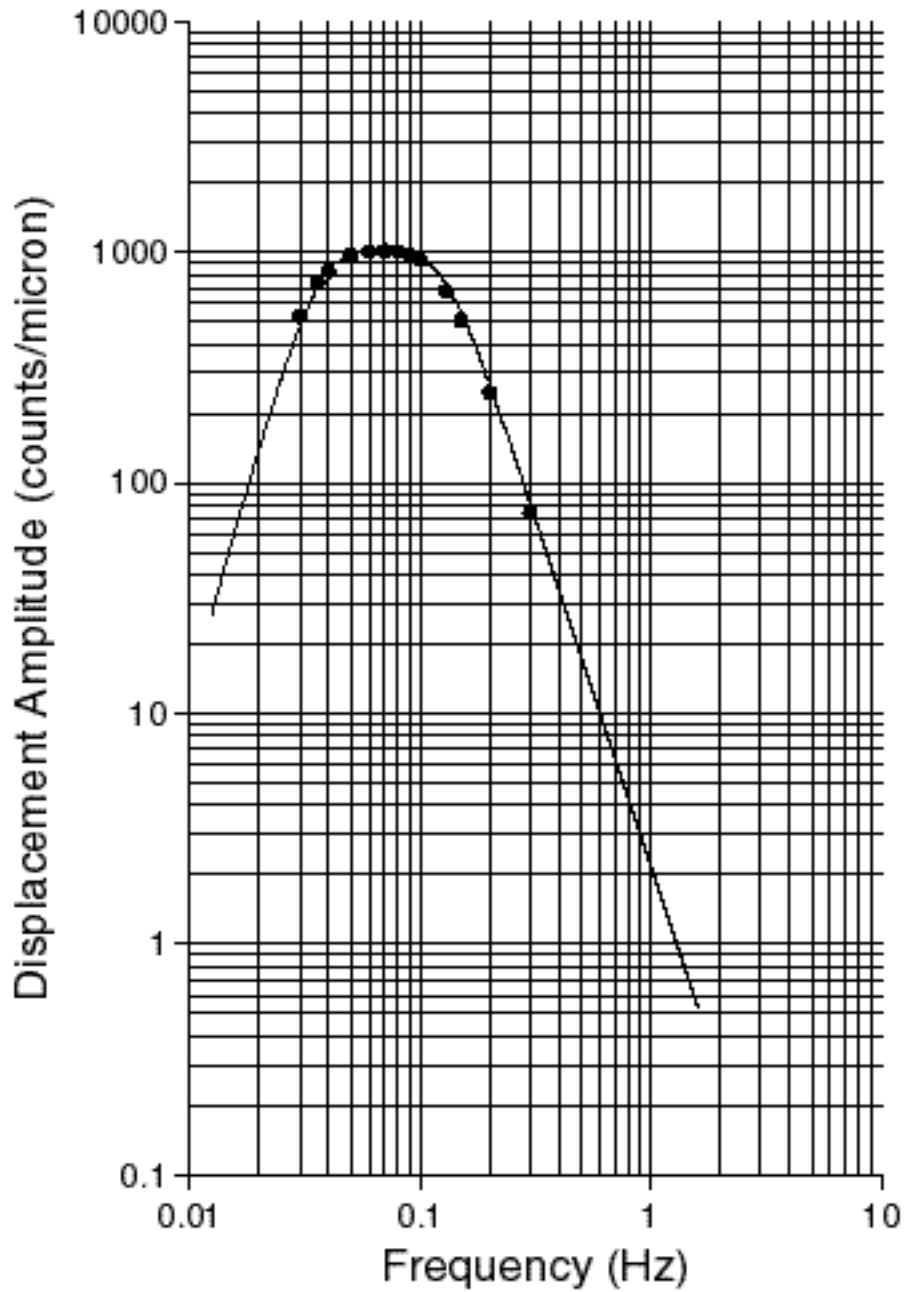
Figure 10: Comparison between the calibration pulses recorded by the vertical component, intermediate-period SV1 seismograph (*thick traces*) and corresponding synthetic calibration pulses (*thin traces*). Synthetics calculated with nominal instrument constants before the calibration pulse waveform inversion (*upper traces*) and the synthetics after the waveform inversion (*lower traces*) are plotted to show the overall fits.
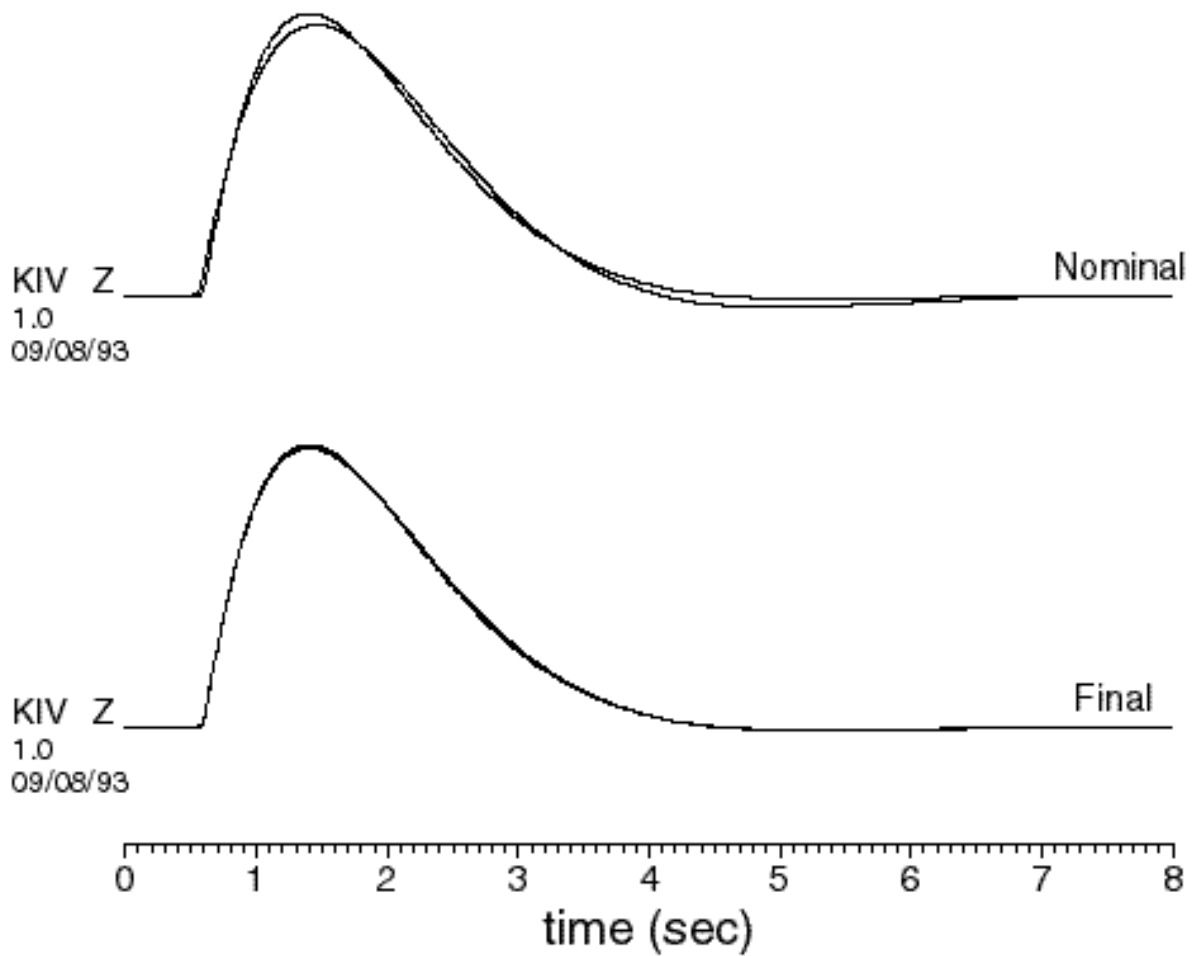
Figure 11: Comparison between the spectral amplitude of the KIV SV1 recorded calibration pulse (*thick line*) and corresponding synthetic calibration pulse after the waveform inversion (*crosses*).

oriented essentially radially) traces are modelled with a point shear dislocation source in the standard Earth model PREM (Dziewonski and Anderson, 1981). The direct P and free surface reflected rays pP and sP, as well as the core-mantle boundary reflected ray PcP are generated using the WKBJ seismogram method (Chapman, 1978). These primary rays are convolved with a simple triangular source time function of 1 second duration, a Futterman attenuation operator with $t^* = 0.5$ sec, and TSG-DS seismograph responses following a standard practice. The double-couple point source mechanisms given in the Harvard CMT catalog are used for the source radiation pattern.

The overall fit of relative amplitudes and durations between the observed and the synthetic phases are good, suggesting that both the source parameters and the instrument response used in the modeling are reasonably good (Fig. 12). The focal depth of this event is determined by matching the arrival times of PcP and surface reflections pP and sP. Detailed interpretation is needed to identify other phases on the observed records, for instance, P to S converted phases at the discontinuities in the upper mantle (*efi gfi* Garnero *et alfi* 1992; Petersen *et alfi* 1993) as well as at the Moho by calculating synthetic seismograms. The broadband nature of BRVK digital records provides an opportunity to study the seismic velocities and discontinuities in the upper mantle beneath Central Asia.

4. Discussion and Conclusion

In our analysis of the BRVK calibration pulses, we had very little initial knowledge of the seismograph system components. This may be a fairly extreme situation, since for many other systems, one may expect to have information about the design of various filters, which would help in the decision on the initial parameterization of the inverse problem. For the TSG system, we were instead forced to use a trial-and-error approach in order to determine the order and type of all components, excluding the seismometer. We have tried essentially all reasonable linear combinations of high- and low-pass filters for each seismograph. For example. a second-order filter is only chosen if a parameterization in terms of two first-order filters produces an insignificant change in the variance reduction. Our trial configurations tended to favor simplicity, where complexity was unwarranted – hence the use of Butterworth filters, when an arbitrary damping produced no significant improvement in the data fit.

Of the seismographs that we have analyzed, the short-period KSM and long-period system DSM produced the best resolved results, suggesting that these channels of data (low- and high-gain) may be of greatest value for future quantitative analysis of BRVK data. However, we expect that all channels (Figure 13) are sufficiently well calibrated to be suited for modern analysis.

Our analysis did not provide information on absolute gains beyond what could have been learned from single-frequency calibration tables kept at BRVK. If for a different system both the calibration current, and the resulting acceleration of the seismometer mass can be determined, the calibration pulse analysis could also yield useful gain information. Our impression, after having studied BRVK calibration logs for several different years, is that the seismometer gains have been stable, and we see no reason to doubt the gains derived from these tables.

While we have here presented the results of the analysis in terms of a damped seismometer and several simple filter freqeuncies and damping coefficients, we have also converted these into a standard poles and zeros representation. These parameters are available from one of
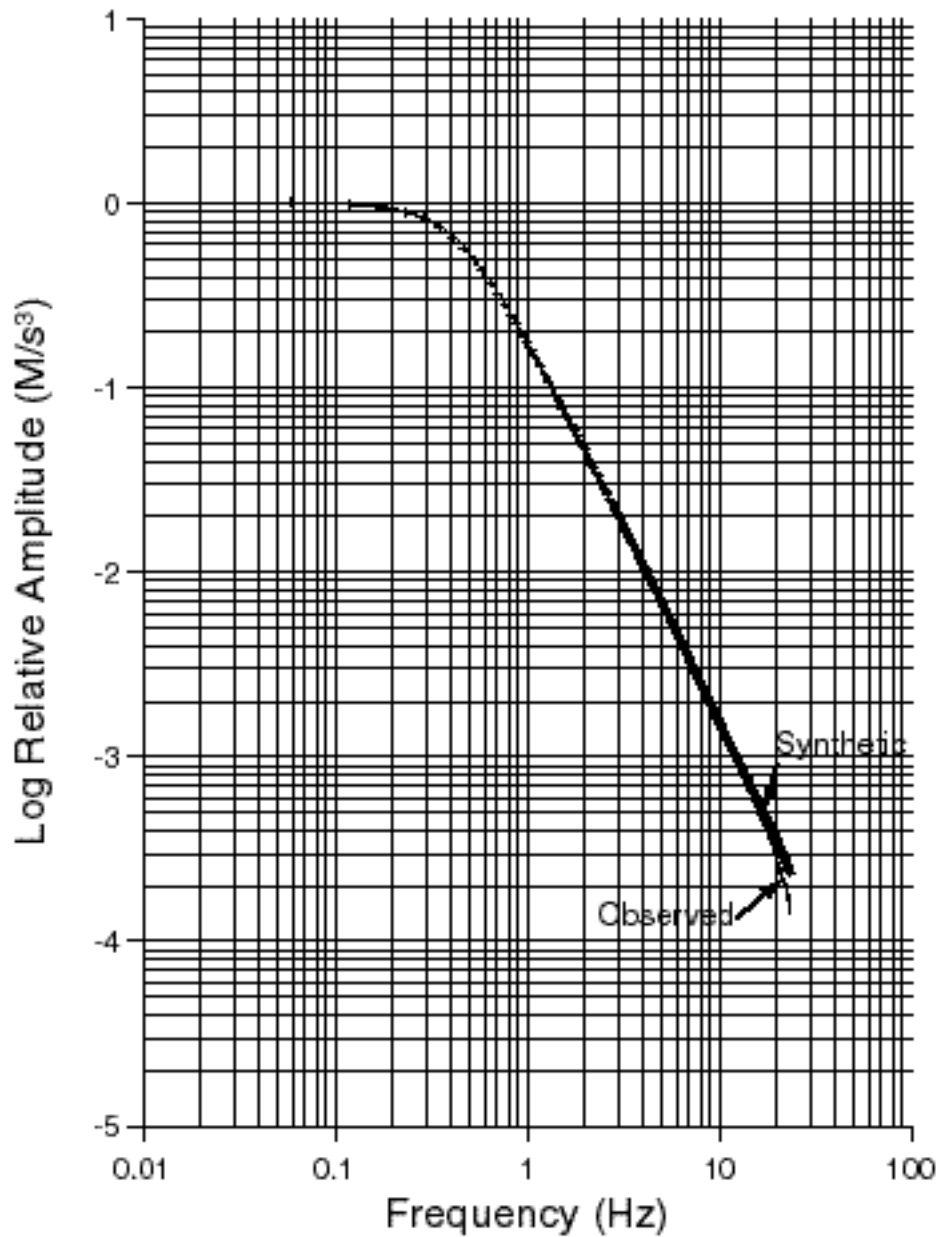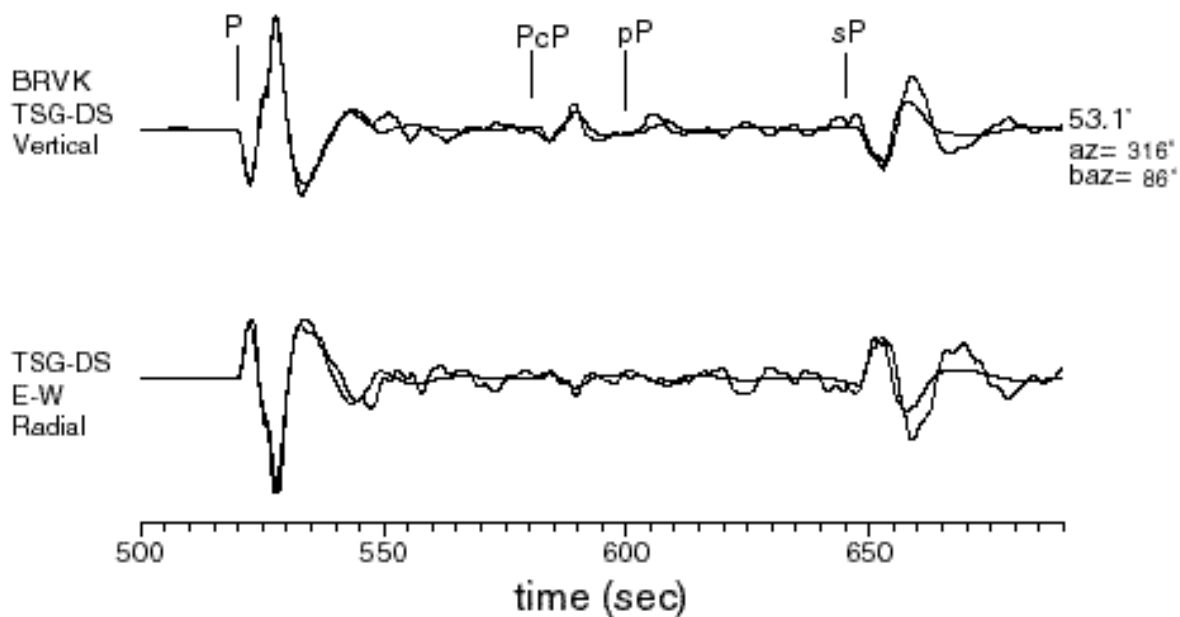
Figure 12: Comparison of vertical and radial (East-West) observed records (*thick traces*) from two deep focus earthquakes with corresponding synthetic seismograms (*thin traces*). (a) deep focus earthquake ($m_b = 6.1$, $h = 400$ km) on 04/24/84 at 04:11 from Southern Honshu, Japan, (b) deep focus earthquake ($m_b = 5.7$, $h = 403$ km) on 04/10/85 at 16:26 from Southern Honshu, Japan.
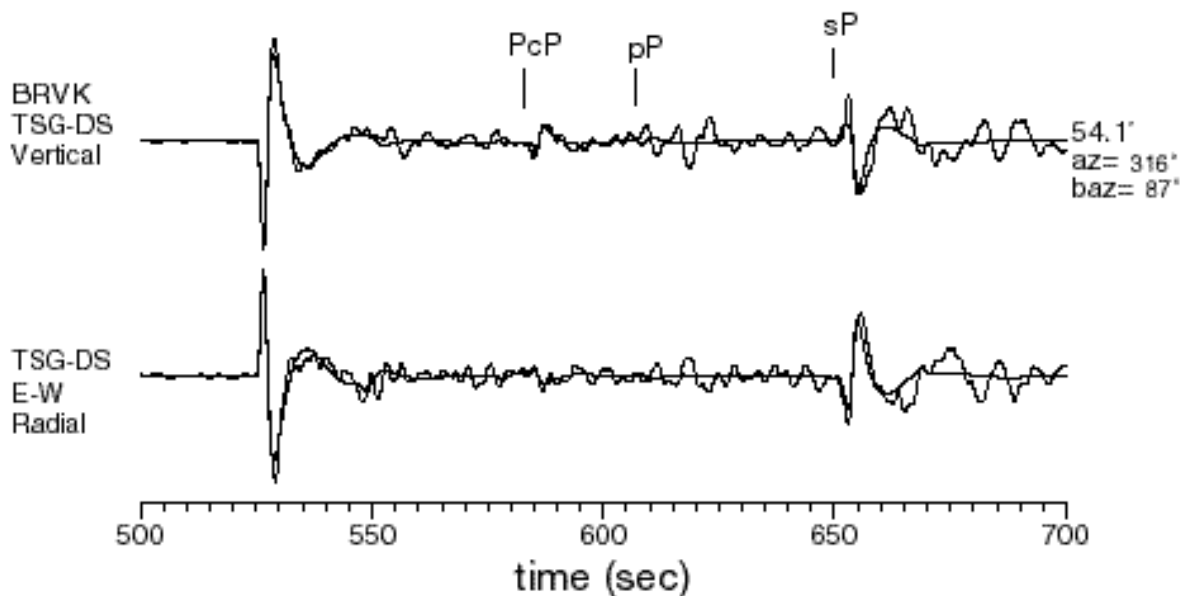
Figure 13: Summary of spectral amplitude responses for all vertical-component seismographs of the TSG system. For each seismograph, frequency-amplitude responses given in the log book at BRVK (*closed circles*) and the amplitude responses obtained after the calibration pulse inversion (*solid lines*) are plotted together for comparison.

us (W.-Y. Kim), and will be incorporated with the BRVK data distributed by the IRIS Data Management Center.

5. Acknowledgments

6. References

Aki, K. and P. G. Richards (1980). *Quantitative Seismologyfi Theory and Methods*, W. H. Freeman & Co., San Francisco, Vol. 1, 557pp.

Abramowitz, M. and I. A. Stegun (1964). *Handbook of Mathematical Functions*, U. S. National Bureau of Standards, Dover Publications, Inc., New York, 1045pp.

Adushkin, V. V. and V. A. An (1990). Seismic observations and monitoring of underground nuclear explosions at Borovoye Geophysical Observatory, *Izvfi Acadfi Scifi USSRfi Physfi Solid Earth*, no. **12**, 1023-1031.

Berger, J. D. W. McCowan, W. E. Farrell and R. T. Lacoss (1978). Comments on "Transfer functions for the seismic research observatory seismograph system" by Douglas McCowan and Richards T. Lacoss, *Bullfi Seismfi Socfi Amfi* **68**, 1537-1538.

Berger, J. D. C. Agnew, R. L. Parker and W. E. Farrell (1979). Seismic system calibration: 2. Cross-spectral calibration using random binary signals, *Bullfi Seismfi Socfi Amfi* **69**, 271-288.

Bolduc, P. M. R. M. Ellis and R. D. Russell (1972). Determination of seismograph phase response from amplitude response, *Bullfi Seismfi Socfi Amfi* **62**, 1665-1672.

Chapman, C. H. (1978). A new method for computing synthetic seismograms, *Geophysfi Jfi Rfi astrfi Socfi* **54**, 481-518.

Choy, G. L. and V. Cormier (1983). The structure of the inner core inferred from short-period and broadband GDSN data, *Geophysfi Jfi Rfi astrfi Socfi* **72**, 1-21.

D'Azzo, J. J. and C. H. Houpis (1975). *Linear Control System Analysis and Designfi Confi ventional and Modern*, McGraw-Hill Inc., New York, 636pp.

Dziewonski, A. M. and D. L. Anderson (1981). Preliminary reference Earth model (PREM), *Physfi Earth Planetfi Interfi* **25**, 297-356.

Farrell, W. E. and J. Berger (1979). Seismic system calibration: 1. Parametric model, *Bullfi Seismfi Socfi Amfi* **69**, 251-270.

Garnero, E. J. D. V. Helmberger and L. J. Burdick (1992). Preliminary observations from the use of US-Soviet Joint Seismic Program data to model upper mantle triplications beneath Asia, *Geophysfi Jfi Intfi* **113**, 252-259.

Graupe, D. (1972). *Identification of Systems*, Van Nostrand Reinhold Co., New York, 276pp.

Hagiwara, T. (1958). A note on the theory of the electromagnetic seismograph, *Bullfi Earthqfi Resfi Instfi* Univ. Tokyo, **36**, 139-164.

Harvey, D. and G. L. Choy (1982). Broad-band deconvolution of GDSN data, *Geophysfi Jfi Rfi astrfi Socfi* **69**, 659-668.

Herrmann, R. B. (1977). On the determination of the impulse response of seismograph systems with emphasis on the SRO system, *Earthquake Notes*, **48**, No. 1-2, 3-23.

Jarosch, H. and A. R. Curtis (1973). A note on the calibration of the electromagnetic seismograph, *Bullfi Seismfi Socfi Amfi* **63**, 1145-1155.

Luh, P. C. (1977). A scheme for expressing instrumental responses parametrically, *Bullfi Seismfi Socfi Amfi* **67**, 957-969.

McCowan, D. W. and R. T. Lacoss (1978). Transfer functions for the seismic research observatory seismograph system, *Bullfi Seismfi Socfi Amfi* **68**, 501-512.

McGonigle, R. W. and P. W. Burton (1980). Accuracy in LP electromagnetic seismograph calibration by least-squares inversion of the calibration pulse, *Bullfi Seismfi Socfi Amfi* **70**, 2261-2273.

Mitchell, B. J. and M. Landisman (1969). Electromagnetic seismograph constants by least-squares inversion, *Bull. Seism. Soc. Am.* **59**, 1335-1348.

Mitronovas, W. (1976). Accuracy in phase determination of LP electromagnetic seismographs based on transient calibration pulse, *Bull. Seism. Soc. Am.* **62**, 97-104.

Petersen, N. L. Vinnik, G. Kosarev, R. Kind, S. Oreshin and K. Stammler (1993). Sharpness of the mantle discontinuities, *Geophys. Res. Lett.* **20**, 859-862.

Richards, P. G. W. Y. Kim and G. Ekström (1992). The Borovoye Geophysical Observatory, Kazakhstan, *EOS*, **73**, 201-206.

Woodward, R. L. and G. Masters (1989). Calibration and data quality of the long-period SRO/ASRO network, 1977 to 1980, *Bull. Seism. Soc. Am.* **70**, 1972-1983.

Table 1. Characteristics of STsR-TSG Seismic System at Borovoye Seismic Station (*).

Seismograph	Data channel	T_S[a] (s)	s[b]	Gain[c] (count/μ)	f_n[d] (Hz)	dt[e] (msec)	Channel[f] number	Vaild[g] date
KS		1.5	0.7	2250	1.5	26	7,8,9	07/23/76 -
		1.5	0.7	4500	1.5	26	7,8,9	03/24/82 -
DS		20.0	0.5	50	0.1	312	19,20,21	07/12/74 -
KSM	HG[h]	1.5	0.35	100000	1.0	26	10,11,12	11/01/81 -
	LG[i]			1000		26	3,4,5	
DSM	HG	28.0	0.5	1000	0.07	312	22,23,24	09/08/82 -
	LG			10		312	15,16,17	
KSVM	HG (Z)[j]	1.5	0.35	4600	1.0	26	2	12/12/83 -
	LG (Z)[j]			50		26	1	

(*) STsR-TSG system from Feb 1973 to present,

(a) T_S = Seismometer natural period in second, (b) s = Seismometer damping constant, (c) Gain = Nominal gain in counts/μ, (d) f_n = normalization frequency where the nominal gain is measured, (e) dt = Sampling interval in millisecond, (f) Channel identifier on the original station tape, (g) dates when the responses given are valid, (h) High-gain channel, (i) Low-gain channel, (j) Only vertical-component.

Table 2. Instrument constants of the STsR-TSG seismographs from inversion [*].

	Seismometer		High pass		Low pass	Rms fit	Actual gain	f_n	Channel number
	T_S (sec)	s	f_H (Hz)		f_L (Hz)		(counts/μ)	(Hz)	
					KS[a] (07/23/76 -)				
			f_{H1}		f_{L1}				
Nominal	1.500	0.70	0.77		5.00	17.272	2250	1.5	7
Z	1.646 (+9.8%)	0.591 (-15.6%)	1.18		4.00	8.562	2240	1.5	7
NS	1.495 (-0.3%)	0.588 (-16.1%)	1.16		4.00	8.263	2279	1.5	8
EW	1.622 (+8.1%)	0.583 (-16.7%)	1.18		4.00	9.891	2183	1.5	9
					KSM[b] (11/01/81 -)				
			f_{H2}	H2	f_{L2}				
Nominal	1.500	0.350	0.650	0.707	8.00	34.521	100000	1.0	10
Z	1.481 (-1.4%)	0.332 (-5.4%)	0.630	1.042	8.13	1.249	100576	1.0	10
NS	1.515 (+1.0%)	0.345 (-1.4%)	0.636	1.049	8.47	1.781	97891	1.0	11
EW	1.520 (+1.3%)	0.349 (-0.3%)	0.644	1.034	8.77	2.365	99279	1.0	12
					KSVM[c] (12/12/83 -)				
			f_{H2}	H2	f_{L3}				
Nominal	1.50	0.350	0.667	0.707	5.00	22.640	4600	1.0	2
		0.356							
Z	1.49 (-0.6%)	0.356 (-1.7%)	0.671	1.056	5.29	7.828	4626	1.0	2

Table 2. Continued. 29

DS (12/01/83 -)

		f_{H2}	H2	f_{L1}	f_{L2}	L2				
Nominal	20.00	0.50	0.029	0.71	0.50	0.57	1.00	43.320	50.0	0.1	19
Z	20.10 (+0.5%)	0.60 (+20%)	0.027	0.79	0.49	0.49	0.77	5.763	48.29	0.1	19
NS	19.13 (-4.4%)	0.50 (+0.6%)	0.027	0.77	0.50	0.49	0.78	6.552	46.78	0.1	20
EW	19.49 (-2.6%)	0.53 (+5.7%)	0.028	0.75	0.52	0.57	0.91	6.130	46.32	0.1	21

DSM[d] (09/08/82 -)

		f_{H1}	f_{H1}	f_{L3}					
Nominal	28.00	0.50	0.017	0.033	0.125	10.630	1000	0.07	22
Z	26.58 (-5.3%)	0.48 (-3.4%)	0.018	0.029	0.130	1.600	992	0.07	22
NS	29.43 (+5.1%)	0.52 (+4.0%)	0.016	0.029	0.130	2.932	1001	0.07	23
EW	27.13 (-3.1%)	0.49 (-2.6%)	0.018	0.030	0.130	4.015	1002	0.07	24

[*] For each seismograph, date is indicated for which the instrument response listed is applicable;

[a] Calibration pulses recorded on 10/14/78 and on 02/04/80 are used. Nominal gain during 07/23/76 - 01/30/82 was 2,250 counts/μ, and the nominal gain since 03/24/82 - present is 4,500 counts/μ;

[b] KSM low-gain channels have identical responses, but with lower gains of Z (3) = 982, NS (4) = 1002, EW (5) = 995;

[c] KSVM low-gain channel has identical response, but with a lower gain of, Z (2) = 46.15;

[d] DSM low-gain channels have identical responses, but with lower gains of, Z (15) = 10.0, NS (16) = 9.9, EW (16) = 10.0.

Table 3. TSG-KSM vertical component inversion result.

Iteration Number	Seismometer		High pass		Low pass	K	Rms fit
	T_S (sec)	s	f_{H1} (Hz)	H1	f_{L2} (Hz)		
	1.500	0.350	0.650	0.707	8.000	1.000	34.521
1	1.477	0.316	0.633	1.012	8.130	1.013	3.427
2	1.480	0.332	0.630	1.042	8.120	1.014	1.265
3	1.481	0.332	0.630	1.042	8.118	1.014	1.249

Table 4. KIV-SV1 vertical-component instrument constants from inversion.

	Seismometer		Low pass	Rms fit
	T_S (sec)	s	f_{H5} (Hz)	
Nominal	5.00	0.707	34.30	44.640
SV1 (Z)	4.64 (-7.8%)	0.809 (+14.4%)	33.80 (-1.5%)	0.014
Modified		0.867 (-7.2%)		